Optics Letters

Impact of modal gain and waveguide design on two-state lasing in quantum well-dot lasers

M. V. Maximov,[1,*] Yu. M. Shernyakov,[2] G. O. Kornyshov,[2] A. A. Beckman,[2] F. I. Zubov,[1] A. A. Kharchenko,[1] A. S. Payusov,[2] S. A. Mintairov,[2] N. A. Kalyuzhnyy,[2] V. G. Dubrovskii,[3] and N. Yu. Gordeev[2]

[1]Alferov University, St. Petersburg 194021, Russia
[2]Ioffe Institute, St. Petersburg 194021, Russia
[3]Faculty of Physics, St. Petersburg State University, St. Petersburg 199034, Russia
*maximov@beam.ioffe.ru

Received 13 June 2024; revised 27 September 2024; accepted 8 October 2024; posted 9 October 2024; published 28 October 2024

We study the current-controlled lasing switching from the ground state (GS) to the excited state (ES) transition in broad-area (stripe width 100 µm) InGaAs/GaAs quantum well-dot (QWD) and quantum well (QW) lasers. In the lasers with one QWD layer and a 0.45 µm-thick GaAs waveguide, pure GS lasing takes place up to an injection current as high as 8 A (40 kA/cm^2). In contrast, in QW lasers with a similar design, ES lasing emerges already at 3 A (15 kA/cm^2). The ES lasing in the QWD lasers is observed only in the devices with a waveguide thickness of 0.78 µm that supports a 2nd order transverse mode at the wavelength of the ES transition. Increasing the modal gain in the lasers with 0.78 µm-thick waveguide by using two QWD layers in the active region suppresses the ES lasing. © 2024 Optica Publishing Group. All rights, including for text and data mining (TDM), Artificial Intelligence (AI) training, and similar technologies, are reserved.

https://doi.org/10.1364/OL.532606

Simultaneous lasing via ground and excited state transitions in quantum dot (QD) and quantum well (QW) lasers has been the subject of intensive research in recent years. It has been experimentally and theoretically shown that even if lasing initially starts via the ground state (GS) transition, the second lasing line at the wavelength corresponding to the excited state (ES) transition can emerge with an increase in the injection current [1–4]. This effect, also referred to as two-state lasing (double-state lasing), is due to a current-induced increase in carrier concentration in the excited state (ES) and their limited relaxation rate from the ES to the GS. At high injection currents, the emission via the GS transition can be completely quenched. Lasing via the ES transition is usually considered an undesirable effect as it limits the output power at the GS transition that stops increasing after the onset of ES lasing. On the other hand, lasers emitting two well-separated wavelengths (dual-wavelength lasers) are promising for remote sensing instruments, laser ranging, topography, and many medical applications [5]. Lasing switching from the GS to ES transitions is strongly pronounced in QD lasers because of the low QD surface density and inhomogeneous broadening of the QD array, which results in a relatively low density of states corresponding to the GS transition [1,2,6,7]. This effect has also been observed in QW lasers, but it occurs at much higher currents than in QD lasers because of the high density of states in QWs [3,4].

In this study, we investigate two-state lasing in InGaAs/GaAs quantum well-dot (QWD) lasers. QWDs represent a very dense array of indium-rich InGaAs islands inside an indium-depleted residual InGaAs QW [8]. They are intermediate in properties between QWs and QDs and can be considered as quantum heterostructures of mixed (0D/2D) dimensionality. In [9], we have studied lasing switching from the GS to the ES transition with a decrease in cavity length (i.e., an increase in external loss). We have shown that the density of states of the InGaAs/GaAs QWDs only slightly increases to higher energies, if at all, which makes it qualitatively different from that of QWs and QDs. A very high material gain for the QWD ground-state transition of $1.1 \times 10^4\,\mathrm{cm}^{-1}$ has been demonstrated [10]. The above-mentioned properties of QWDs make it possible to maintain ground-state lasing near the threshold in shorter cavities (higher output loss) as compared to the QW lasers emitting in the same optical range [9]. In this paper, we study in detail the lasing switching between the GS and ES transitions in the QWD lasers as injection current increases depending on the modal gain, optical confinement factor (transverse waveguide design) and cavity length.

We have fabricated and studied four types of QWD-based lasers and a reference QW-based laser. In the QWD lasers, the number of QWD layers in the active region is either one or two. A GaAs waveguide thickness has been chosen either 0.45 µm (narrow waveguide - NWG) or 0.78 µm (broad waveguide - BWG). Thus, there are four types of QWD lasers under study that we refer to as 1QWD NWG, 1QWD BWG, 2QWD NWG, and 2QWD BWG. Laser heterostructures with an active region based on QWDs have been grown by metal-organic vapor-phase epitaxy (MOVPE) on n+-GaAs substrates misoriented by 6° towards the [111] direction. The QWDs have been formed by the deposition of an $In_{0.4}Ga_{0.6}As$ layer with a nominal thickness of ~2.4 nm (eight monolayers) [8]. The use of misoriented substrates facilitates the formation of the QWDs. In case of 2QWD NWG and 2QWD BWG lasers, the QWD layers in the active

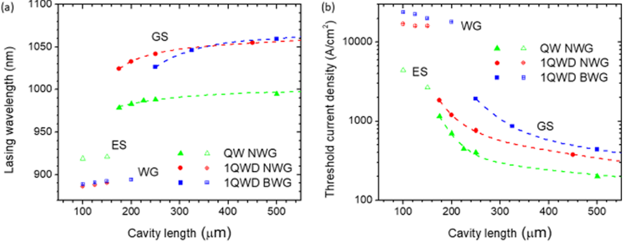

Fig. 1. (a) Lasing wavelength and (b) threshold current density versus the cavity length for the QW NWG, 1QWD NWG, and 1QWD BWG lasers. GS, ES, and WG denote lasing via the ground state (solid symbols), excited state (open symbols), and GaAs waveguide (open with a cross symbols), respectively.

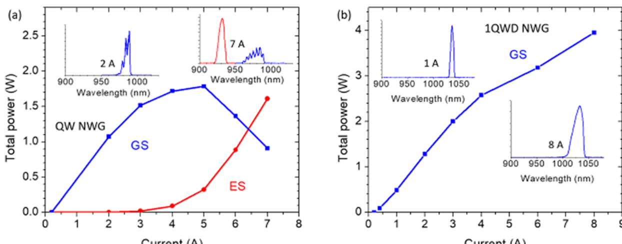

Fig. 2. Light–current characteristics of (a) the 0.2 mm long QW NWG and (b) the 1QWD NWG lasers corresponding to the ground (blue curve) state and excited state (red curve) transitions. The insets show the lasing spectra.

region have been separated using a 40 nm thick GaAs spacer. A reference laser wafer with an active region based on a 6 nm thick $In_{0.2}Ga_{0.8}As$ QW has been grown on an exactly oriented (100) n + -GaAs substrate.

The QWD lasers with the BWG comprise 0.78 μm-thick GaAs waveguide and 1.5 μm-thick p- and n-type $Al_{0.4}Ga_{0.6}As$ claddings. The optical confinement factors (Γ-factor) for the 1QWD and 2QWD lasers with the BWGs have been calculated using the nominal thickness of the QWD layer and amounts to 3.7×10^{-3} and 7.4×10^{-3}, respectively. The QWD lasers with the NWG comprise 0.45 μm-thick GaAs waveguide, 1.45 μm-thick n-type $Al_{0.25}Ga_{0.75}As$ cladding and 1.0 μm-thick p-type $Al_{0.25}Ga_{0.75}As$ cladding. The Γ-factors for the 1QWD and 2QWD lasers with the NWGs are 4.5×10^{-3} and 9.0×10^{-3}, respectively. The difference in Al composition of the cladding layers in QWD NWG and QWD BWG lasers does not affect the growth of QWDs and only 1.1 times increases Γ-factor of the QWD NWG lasers. The reference QW laser with NWG (QW NWG) comprise 0.32 μm-thick GaAs waveguide, and 1.5 μm-thick p- and n-type $Al_{0.4}Ga_{0.6}As$ claddings; its Γ-factor is 1.9×10^{-2}. In all the lasers, the active regions are placed in the center of the GaAs waveguides.

Epitaxial wafers of all types have been processed into broad-area (stripe width 100 μm) lasers using standard optical lithography, reactive-ion etching, deposition of dielectric coatings, and metal contacts. Devices with various cavity lengths and uncoated facets have been cleaved and mounted onto copper heat sinks using indium solder. The mounted devices have been characterized in a pulsed regime (200 ns, 1 kHz) to avoid the overheating caused by the injection current. The current source provides rectangular pulses with pulse fronts of approximately 10 ns. For all the lasers, the maximal injection current in the experiments has been limited by the catastrophic degradation of the laser characteristics.

First, we have studied the threshold current density and the lasing wavelength measured just above the threshold depending on the cavity length L. Figure 1 shows these dependencies for the lasers with one QWD layer and for the reference QW laser. If the cavity length is sufficiently large, lasing occurs in the optical region that corresponds to the transition between the first electron level and the first level of heavy holes in QWs and QWDs (GS transition). With a decrease in the cavity length, the output loss increases, and the GS transition gain eventually becomes lower than the total loss, which results in a lasing switching to transitions with larger optical gain at higher energies, accompanied by an increase in the threshold current density and a lasing wavelength blueshift. For each type of the lasers, there is a minimal cavity length L^{GS}_{min} where the lasing still occurs via the GS transition. We note that the values of L^{GS}_{min} have been experimentally determined with a precision of a few tens of microns because we have measured a limited number of devices.

In the case of the QW active region, the lasing wavelength switches to the transition between the second electron level and the second level of heavy holes [11] when $L \leq 150$ μm [Fig. 1(a)]. We will refer to this transition (920 nm) as to the ES transition in the QW in order to use the same terminology for both QW and QWDs. This scenario is similar to the case of QD lasers in which the emission wavelength sequentially hops to the first and then to the second ES transition with cavity shortening [12]. In contrast, in the QWD lasers, the emission wavelength immediately jumps to the states of the GaAs waveguide bypassing the ES [Fig. 1(a)]. Such behavior near the threshold is caused by the unique density of states of the QWD lasers [9]. For the 1QWD NWG lasers, L^{GS}_{min} is smaller (175 μm) than that of the 1QWD BWG lasers ($L^{GS}_{min} = 250$ μm). We attribute this fact to the higher Γ-factor of the 1QWD NWG laser as compared to the 1QWD BWG one. The 2QWD NWG lasers show the GS lasing down to the shortest cavities studied (100 μm). In the 2QWD BWG lasers, the $L^{GS}_{min} = 125$ μm, and the devices with a shorter cavity ($L = 100$ μm) show lasing via the GaAs waveguide. For the same cavity lengths, the threshold current densities of the lasers with the BWG are higher than those of the NWG lasers. This is explained by the large optical confinement factors and, correspondingly, by the higher modal gain of the QWD lasers with the NWG.

The two-state lasing has been investigated over a wide range of injection currents ≤12 A for devices with different cavity lengths. All types of the lasers with $L \geq 300$ μm show pure GS lasing up to highest current. A decrease in the cavity length causes an increase in the threshold current density for the GS lasing and an increase in the ES population. Unlike the case of QWs, high energy (ES) transition in QWDs is attributed to the recombination of electrons from the first level and light holes [13,14]. The growth of the carrier population at high energy levels leads to a decrease in the additional current (in excess of the GS threshold) required to achieve the ES lasing. Consequently, some devices with $L \leq 250$ μm show simultaneous lasing via the GS and ES transitions at high injection current density.

Figure 2 compares the light–current characteristics (the dependence of the total output power from two facets on the current) of the 0.2 mm long reference QW NWG and 1QWD NWG lasers. In the case of the QW laser with the NWG [Fig. 2(a)],

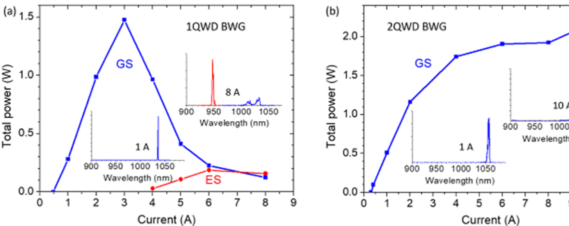

Fig. 3. Light–current characteristics of (a) the 0.25 mm long 1QWD BWG laser and (b) the 0.20 mm long 2QWD BWG laser corresponding to the ground state (blue curve) and excited state (red curve) transitions. The insets show lasing spectra.

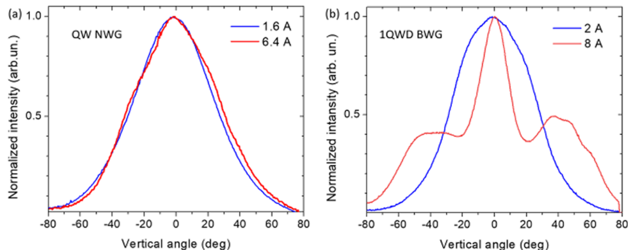

Fig. 4. Transverse far-field patterns of (a) the 0.20 mm long reference QW NWG laser and (b) the 0.25 mm long 1QWD BWG laser at different injection currents.

the intensity of the GS lasing linearly increases with an increase in the current (I) from the threshold value of 0.2 A (current density $J = 1$ kA/cm^2) to ~3 A (15 kA/cm^2). At this injection current, the ES transition lasing line emerges at 930 nm. A further increase in the current results in a sublinear growth, the following rollover of the GS lasing intensity, and rapid growth of the ES one. The sublinear growth and the rollover can be explained by the joint contribution of two effects: non-instantaneous carrier relaxation from the GaAs waveguide to the QW ground state and current-induced growth of the internal optical loss [15,16]. In QD lasers, the quenching of the GS emission intensity after the beginning of the ES lasing earlier has been explained by the difference in the electron and hole capture rates into the QDs together with the fact that hole levels are closely spaced [7]. There is broadening of the GS transition lasing line, where the full width at half maximum (FWHM) grows from 4.2 to 14.5 nm with an increase in I from 0.2 to 7 A. A significant increase in the width of the lasing spectrum is typical of QD lasers [17] as more and more QDs in the inhomogeneously broadened QD array are filled with carriers when the current increases and starts participating in the lasing. The intensity of the GS transition lasing peak is strongly modulated [see the inset in Fig. 2(a)], which is ascribed to the mode-grouping effect [18]. In contrast, in the 1QWD laser with the NWG [Fig. 2(b)], there is no lasing corresponding to the ES transition up to $I = 8$ A ($J = 40$ kA/cm^2). Thus, GS lasing is maintained in the QWD devices up to much higher injection currents than in the QW ones.

The 0.25 mm long QW NWG and 1QWD NWG lasers show characteristics qualitatively similar to that of the 0.20 mm long ones. The QW NWG laser exhibits two-state lasing at $I > 6$ A ($J > 24$ A/cm^2). The 1QWD NWG laser demonstrates pure GS lasing (no emission from the ES transition) up to 12 A (48 kA/cm^2).

The behavior of the 1QWD lasers with the BWG [Fig. 3(a)] is quite different from that of the 1QWD lasers with the NWG [Fig. 2(b)]. We have investigated 1QWD BWG lasers with a cavity length of 0.25 mm because this is the shortest cavity where lasing starts via the GS transition at threshold [Fig. 1]. In the injection current range of 0.5–4 A, lasing proceeds only via the GS transition; its intensity grows linearly in the current range of 0.5–3 A and then decreases [Fig. 3(a)]. Lasing via the ES transition at 960 nm begin at $I = 4$ A ($J = 16$ kA/cm^2). With the further increase in I from 4 to 8 A, the intensity of the GS lasing continues to decrease. The intensity of the ES lasing first increases linearly, and at $I > 6$ A it does not change. The FWHM of the GS transition lasing line increases over the entire range of the injection currents and reaches 36 nm at 8 A.

Using the second QWD layer in the active region dramatically changes the characteristics of the lasers with the BWG. Figure 3(b) shows the light–current curve of a 0.2 mm long 2QWD BWG laser. The cavity length has been chosen to compare the device characteristics with those of the lasers with NWG, as shown in Fig. 2.

The 2QWD BWG laser, which has twice the modal gain, demonstrates pure GS lasing up to $I = 10$ A ($J = 50$ kA/cm^2) despite the fact that its cavity length is shorter than that of the 1QWD BWG laser in Fig. 3(a). Thus, the ES lasing can be suppressed by increasing the modal gain.

Figure 4(a) shows the transverse far-field patterns of the QW NWG laser characterized by a nearly Gaussian shape. This implies that the laser operates in the fundamental transverse optical mode over the entire range of the injection current, even at values corresponding to the ES lasing. An increase in the injection current with corresponding lasing switching to the ES transition causes only a minor broadening of the far-field, which is likely due to the current-induced change in the refractive indices [19]. All the lasers under study, except the 1QWD BWG one, show one-lobe far-field patterns with a nearly Gaussian shape. In contrast, the 1QWD laser with the BWG demonstrated a qualitatively different far-field pattern behavior [Fig. 4(b)]. At the current ranging from the GS lasing threshold to the ES lasing onset at 4 A, the far-field pattern shows a broad lobe of 57° FWHM; the device operates mainly in the fundamental optical mode. However, starting from the ES lasing onset, there are 3 well-resolved lobes in the far-field, which manifests lasing on the 2nd order transverse mode. This effect can be explained by the fact that owing to the dispersion of the refractive indices, the BWG has different sets of allowed transverse optical modes in the ES and GS wavelength ranges. In the GS wavelength range, the BWG thickness is below the 2nd order mode cutoff, whereas in the ES wavelength range, it exceeds the cutoff. The fundamental transverse mode possesses a higher Γ-factor but lower facet reflectivity than the 2nd order mode [20]. This combination causes the 1QWD BWG lasers to operate on the 2nd order mode [Fig. 4(b)]. Note that in the case of the QWD active region, the ES lasing can be achieved only if it is facilitated by the existence of a high-order traverse mode in the BWG. In contrast, the QW lasers exhibit the ES lasing in the NWG.

Figure 5 compares the temperature dependencies of the GS and ES threshold current densities (J_{th}^{GS} and J_{th}^{ES}, respectively) of the reference QW and 1QWD BWG lasers. The first shows the GS lasing up to 58°C [Fig. 5(a)]. At 60°C, the GS emission quenched, and above this temperature, only the ES lasing is observed. The J_{th}^{GS} quickly grows with increasing temperature (characteristic temperature $T_0 = 28$ K), which is typical for

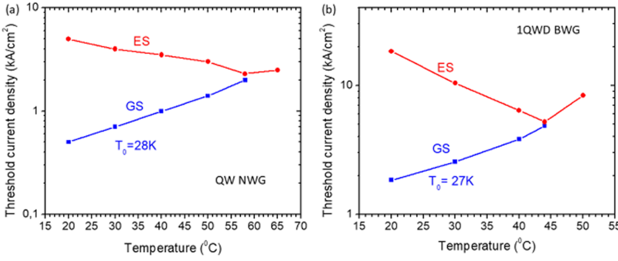

Fig. 5. Temperature dependencies of the GS and ES threshold current densities (J_{th}^{GS} and J_{th}^{ES}, respectively) of (a) the 0.20 mm long reference QW NWG laser and (b) the 0.25 mm long 1QWD BWG laser.

semiconductor lasers with a high output loss (short cavities). In contrast, J_{th}^{ES} decreases in this temperature interval, which can be explained by the higher carrier population of the ES at elevated temperatures and correspondingly smaller additional current required to achieve the J_{th}^{ES} [21]. The J_{th}^{ES} starts increasing after the GS lasing quenching. The J_{th}^{GS} and J_{th}^{ES} of the 1QWD BWG laser [Fig. 5(b)] exhibit qualitatively similar behavior to the corresponding characteristics of the QW NWG one. However, the GS lasing quenches at a lower temperature (44°C), which we attribute to the higher threshold current density of the 1QWD BWG laser and correspondingly higher ES population at the GS threshold.

In conclusion, we have demonstrated that QWD lasers with a short resonator can stably operate on GS states without switching to ES states up to very high current density of 40 kA/cm^2. This makes QWD edge-emitting lasers promising for applications that require ground-state lasing in short cavities, for instance, for high-speed devices. The use of only one active layer facilitates low threshold current in such lasers. On the other hand, two-state lasing can be useful in certain applications, such as dual-wavelength semiconductor lasers [22]. The threshold of two-state lasing can be controlled by the modal gain (number of QWD layers in the active region and design of the transverse waveguide) and temperature. The possibility of current-controlled switching of the lasing wavelength and far-field pattern can be utilized in modulators, sensors, neuromorphic photonic integrated circuits [23], and for data transmission [24].

Funding. Ministry of Science and Higher Education of the Russian Federation (FSRM-2023-0010); Saint Petersburg State University (95440344).

Disclosures. The authors declare no conflicts of interest.

Data availability. Data underlying the results presented in this paper are not publicly available at this time but may be obtained from the authors upon reasonable request.

REFERENCES

1. A. E. Zhukov, A. R. Kovsh, D. A. Livshits, *et al.*, Semicond. Sci. Technol. **18**, 774 (2003).
2. A. Markus, J. X. Chen, C. Paranthoën, *et al.*, Appl. Phys. Lett. **82**, 1818 (2003).
3. D. A. Veselov, K. R. Ayusheva, N. A. Pikhtin, *et al.*, J. Appl. Phys. **121**, 163101 (2017).
4. K. Vizbaras, K. Kashani-Shirazi, and M.-C. Amann, Appl. Phys. Lett. **95**, 071107 (2009).
5. B. M. Walsh, Laser Phys. **20**, 622 (2010).
6. L. V. Asryan, M. Grundmann, N. N. Ledentsov, *et al.*, IEEE J. Quantum Electron. **37**, 418 (2001).
7. V. V. Korenev, A. V. Savelyev, M. V. Maximov, *et al.*, Appl. Phys. Lett. **111**, 132103 (2017).
8. M. V. Maximov, A. M. Nadtochiy, S. A. Mintairov, *et al.*, Appl. Sci. **10**, 1038 (2020).
9. M. V. Maximov, N. Y. Gordeev, A. S. Payusov, *et al.*, Laser Phys. Lett. **17**, 095801 (2020).
10. N. Y. Gordeev, M. V. Maximov, A. S. Payusov, *et al.*, Semicond. Sci. Technol. **36**, 015008 (2020).
11. D. A. Vinokurov, S. A. Zorina, V. A. Kapitonov, *et al.*, Semiconductors **41**, 1230 (2007).
12. M. V. Maximov, L. V. Asryan, Y. M. Shernyakov, *et al.*, IEEE J. Quantum Electron. **37**, 676 (2001).
13. N. N. Ledentsov, D. Bimberg, Y. M. Shernyakov, *et al.*, Appl. Phys. Lett. **70**, 2888 (1997).
14. S. A. Mintairov, N. A. Kalyuzhnyi, M. V. Maksimov, *et al.*, Tech. Phys. Lett. **46**, 203 (2020).
15. L. V. Asryan, Appl. Phys. Lett. **88**, 073107 (2006).
16. Z. N. Sokolova, N. A. Pikhtin, and L. V. Asryan, J. Lightwave Technol. **36**, 2295 (2018).
17. A. Kovsh, I. Krestnikov, D. Livshits, *et al.*, Opt. Lett. **32**, 793 (2007).
18. E. P. O'Reilly, A. I. Onischenko, E. A. Avrutin, *et al.*, Electron. Lett. **34**, 2035 (1998).
19. K. J. Beernink, J. J. Alwan, and J. J. Coleman, Appl. Phys. Lett. **58**, 2076 (1991).
20. I. A. Kostko, V. P. Evtikhiev, E. Y. Kotel'nikov, *et al.*, Semiconductors **33**, 693 (1999).
21. M. V. Maximov, Y. M. Shernyakov, F. I. Zubov, *et al.*, Semicond. Sci. Technol. **28**, 105016 (2013).
22. C.-C. Huang, C.-H. Cheng, Y.-S. Su, *et al.*, IEEE Photonics Technol. Lett. **16**, 371 (2004).
23. C. Mesaritakis, A. Kapsalis, A. Bogris, *et al.*, Sci. Rep. **6**, 39317 (2016).
24. M. V. Maximov, Y. M. Shernyakov, N. Y. Gordeev, *et al.*, Phys. Scr. **98**, 125119 (2023).